Journal of Medicinal Chemistry

Article

pubs.acs.org/jmc

Virtual Screening Identifies Novel Sulfonamide Inhibitors of *ecto*-5′-Nucleotidase

Peter Ripphausen,[†] Marianne Freundlieb,[‡] Andreas Brunschweiger,[‡,∥] Herbert Zimmermann,[§] Christa E. Müller,*[,‡] and Jürgen Bajorath*[,†]

[†]Department of Life Science Informatics, B-IT, LIMES Program Unit Chemical Biology and Medicinal Chemistry, Rheinische Friedrich-Wilhelms-Universität, Dahlmannstrasse 2, D-53113 Bonn, Germany

[‡]PharmaCenter Bonn, Pharmaceutical Institute, Pharmaceutical Chemistry I, University of Bonn, An der Immenburg 4, D-53121 Bonn, Germany

[§]Institute of Cell Biology and Neuroscience, Biologicum der J. W. Goethe—Universität Frankfurt, Frankfurt am Main, Germany

Supporting Information

ABSTRACT: We aimed to identify inhibitors of *ecto*-5′-nucleotidase (*ecto*-5′-NT, CD73), a membrane-bound metallophosphoesterase that is implicated in the control of purinergic receptor signaling and a number of associated therapeutically relevant effects. Currently, only very few compounds, including ADP, its more stable analogue α,β-methylene-ADP, ATP, and anthraquinone derivatives are known to inhibit this enzyme. In the search for inhibitors with more drug-like properties, we applied a model structure-based virtual screening approach augmented by chemical similarity searching. On the basis of this analysis, 51 candidate compounds were finally selected for experimental evaluation. A total of 13 of these molecules were confirmed to have competitive inhibitory activity. The most potent inhibitor, 6-chloro-2-oxo-*N*-(4-sulfamoylphenyl)-2*H*-chromene-3-carboxylic acid amide (**17**), showed an IC_{50} value of 1.90 μM. In contrast to the nucleotide- and anthraquinone-derived antagonists, the newly identified competitive inhibitors are uncharged at physiological pH values, possess a drug-like structure, and are structurally distinct from known active compounds.

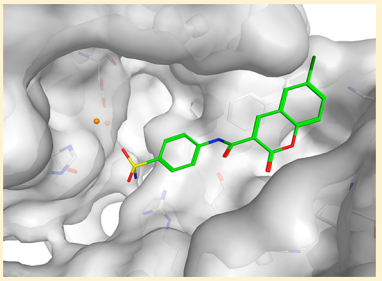

INTRODUCTION

ecto-5′-Nucleotidase (*ecto*-5′-NT, CD73) belongs to a superfamily of metallophosphoesterases containing a dinuclear metal center.[1,2] The enzyme hydrolyzes AMP to adenosine and phosphate.[1,2] However, *ecto*-5′-NT shows no activity toward nucleoside 2′- and 3′-monophosphates. The hydrolysis of 5′-AMP is stereoselective (i.e., only the D- but not the L-enantiomer is a substrate). The K_m values for 5′-AMP (the best substrate) is in the low micromolar range.[3] The enzyme consists of two domains and is connected via a GPI anchor to the extracellular membrane. In a cascade involving ATP- and ADP-hydrolyzing *ecto*-nucleotidases, ATP is hydrolyzed to AMP and thus prevented from acting on P2X and P2Y receptors.[4] The final step is the hydrolysis of AMP by *ecto*-5′-NT thereby increasing the extracellular concentration of adenosine. The nucleoside exhibits neuromodulatory effects through activation of adenosine (P1 purinergic) receptors,[1,2] which play an important role in a variety of therapeutically relevant biological processes.[5] Among others, adenosine exhibits sedative, anticonvulsive, anti-inflammatory, immunosuppressive, antilipolytic, negative inotropic, dromotropic, and chronotropic, vasodilatory, and antidiuretic effects.[6] *ecto*-5′-NT has been found to be upregulated in inflamed tissues.[7−9] Furthermore, many tumor cells express increased levels of *ecto*-5′-NT, thereby producing adenosine that inhibits T cells and promotes angiogenesis. Consequently, antibodies against *ecto*-5′-NT or genetic ablation of the enzyme have been shown to reduce cancer growth and metastasis.[10−13] Accordingly, specific inhibitors of *ecto*-5′-NT are expected to negatively modulate adenosine-dependent signaling pathways and associated effects and are thought to have considerable potential for therapeutic intervention.

Interestingly, ADP and ATP are competitive inhibitors of the enzyme, with inhibition constants that are also in the low micromolar range. It is likely that ADP and ATP bind in a substrate-analogous manner to the active site of *ecto*-5′-NT. However, these natural compounds cannot be hydrolyzed. In in vitro as well as in vivo studies, the more stable α,β-methylene-ADP (AMPCP or AOPCP) is often used as an inhibitor of *ecto*-5′-NT. In addition to adenosine di- and triphosphate (and close analogues), only anthraquinone derivatives are currently known to potently inhibit *ecto*-5′-NT.[14] However, all of these compounds feature at least one strongly acidic function including phosphate groups in the nucleotides and nucleotide analogues or a sulfonate group in the anthraquinone derivatives, which will be deprotonated at physiological pH values. Hence, these compounds will not be able to cross biological barriers, e.g., intestinal membranes or the blood−brain barrier, and thus do not possess properties required for oral drug molecules.

Received: May 10, 2012
Published: June 25, 2012

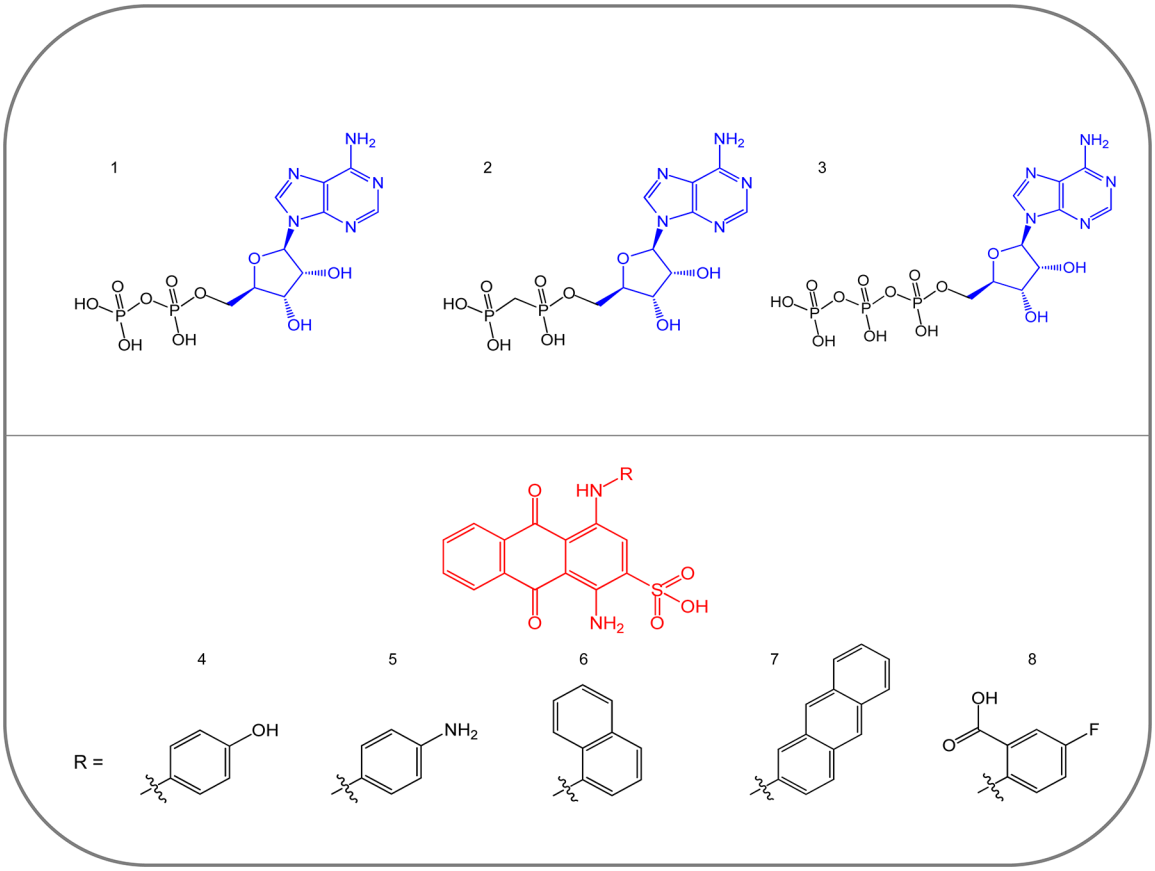

Figure 1. Known inhibitors of *ecto*-5′-NT. Shown are nucleotides and anthraquinone derivatives known to inhibit *ecto*-5′-NT. These compounds were also used as references for similarity searching to preselect database compounds for further analysis. Compounds **1** (ADP) and **3** (ATP) are physiological inhibitors, *β*-methylene-ADP (**2**) is an ADP analogue with increased metabolic stability, and compounds **4**−**8** are anthraquinone derivatives.

Figure 1 shows the structures of representative *ecto*-5′-NT inhibitors. Given the lack of potent, drug-like inhibitors of *ecto*-5′-NT, we have applied a computational screening strategy to search for novel active compounds, leading to the identification of a set of new competitive inhibitors, as reported herein.

RESULTS

Virtual Screening. A total of 70000 preselected test compounds were flexibly docked into a comparative model of *ecto*-5′-NT. A major determinant for the outcome of the virtual screening campaign has been the quality of the model in the active site region of *ecto*-5′-NT. In its active site, the enzyme contains a coordination sphere with two zinc cations that is conserved in the structural template. Zinc cations complex the phosphate groups of the natural substrate AMP. Furthermore, in the active site region, the model was indicated to be a reasonably accurate approximation of the *ecto*-5′-NT structure because the residues forming the active sites in the template and *ecto*-5′-NT were mostly identical, with only four exceptions, i.e., Phe481 (template)/Tyr502 (*ecto*-5′-NT), Arg345/Ala352, Trp277/Phe285, and His240/Asn247. The only nonconservative mutation in the active site region was the Arg345/Ala352 change. However, Arg345 maps to a partly solvent-exposed position in the X-ray structure of the template. Hence, significant conformational effects as a consequence of this mutation were unlikely. In addition, another relevant aspect for virtual screening has been that the nucleoside ligand-bound geometry of the active site of the template structure was transferred to the model. Thus, conserved regions within the active site were present in a conformational state adapted to ligand binding.

Selection of Candidate Compounds. Following docking and a first-path visual inspection for an overall reasonable active site fit, a total of 372 candidate compounds from ZINC-8 remained for further analysis. In the analysis of the hypothetical binding modes of these compounds, three selection criteria were applied: (1) absence of short contacts or steric constraints, (2) presence of possible polar or charge interactions with the active site zinc ions, and (3) presence of aromatic/stacking interactions with Phe 419 and Tyr 512 of *ecto*-5′-NT. These two residues line the major hydrophobic substrate binding region of the enzyme. Figure 2 shows the putative binding mode of one of the test compounds (**17**) in the active site of *ecto*-5′-NT. A total of 128 compounds met these selection criteria, 51 of which could be acquired from commercial sources for testing. Supplier information for each active compound is provided in Table S1 of the Supporting Information.

Experimental Evaluation. The compounds were tested in a radioactive in vitro enzyme assay using [^{3}H]AMP as a substrate. All solutions were carefully monitored to avoid artifacts due to precipitation or agglomeration of compounds. Under assay conditions, aggregation of active compounds was not detectable. In addition, none of these compounds had protein-reactive groups. Significant inhibitory activity was detected for a total 13 of these compounds with IC_{50} values

dx.doi.org/10.1021/jm300658n | J. Med. Chem. 2012, 55, 6576−6581

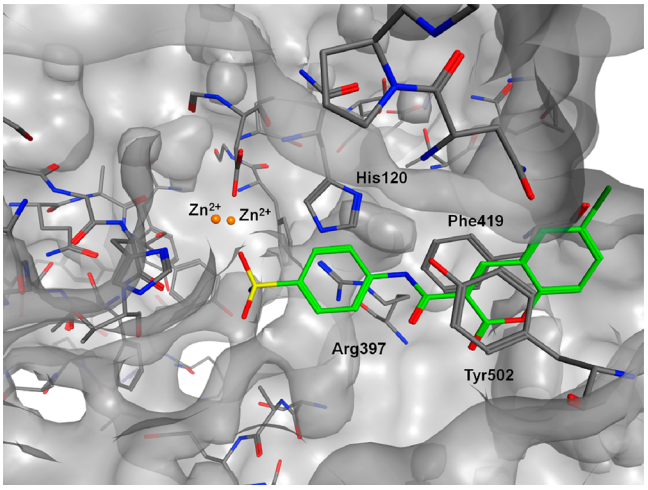

Figure 2. Putative *ecto*-5′-NT/inhibitor complex. Shown is the hypothetical binding mode of compound **17** in the active site of *ecto*-5′-NT including selected residues that might be important for the interaction. The *ecto*-5′-NT model is displayed with a clipped transparent surface. Carbon atoms of compound **17** and *ecto*-5′-NT residues are colored green and gray, respectively. Oxygen atoms are colored in red, nitrogen atoms in blue, and sulfur atoms in yellow. The two catalytic zinc ions in the active site are represented as small spheres (gold).

ranging from 1.90 to 74.8 μM. Their structures, IC_{50} values, and purity information are provided in Table 1. In addition, original docking ranks prior to visual inspection and candidate selection are provided in Table S1 of the Supporting Information.

The inhibitors were structurally diverse, but most of them contained sulfonamide groups.

Six compounds had IC_{50} values below 10 μM, and their inhibition curves are shown in Figure 3. Inhibition curves of all potent compounds are shown in Figure S1 of the Supporting Information. All of these six inhibitors contained sulfonamide groups thought to interact with the zinc coordination sphere of *ecto*-5′-NT (Figure 2). Among these inhibitors was compound **17**, the most potent inhibitor identified in our study, with an IC_{50} value of 1.90 μM corresponding to a K_i value of 1.58 μM. Compound **17** was demonstrated to exert a competitive mechanism of inhibition, as shown in Figure 4.

DISCUSSION

ecto-5′-NT is implicated in a number of therapeutically relevant scenarios. Among other effects, the enzyme is upregulated by HIF-1 in response to oxygen starvation of growing tumor tissues and increases the level of extracellular adenosine, which is a stimulus for angiogenesis. Because extracelluar adenosine is immunosuppressive, *ecto*-5′-NT reduces immune responses to cancer cells.[10−13] Therefore, novel *ecto*-5′-NT inhibitors should merit consideration as potential anticancer and antimetastatic agents.

To date, known potent *ecto*-5′-NT inhibitors only include natural nucleotides and their analogues as well as anthraquinone derivatives. Although both compound series provide valuable tools to investigate the role of *ecto*-5′-NT in purinergic signaling, their potential for pharmaceutical development is likely to be limited. Nucleotides have essential physiological functions and are susceptible to extensive metabolism. Moreover, both nucleotides and sulfoanthraquinone derivatives that show *ecto*-5′-NT inhibition are strongly acidic molecules

Table 1. Structures, Activity, And Purity of New Inhibitors of *ecto*-5′-NT

Compound number	Chemical structure	IC_{50} ± SEM (μM)	Purity[a]
9	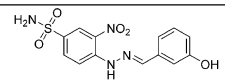	**18.4** ± 1.7	99.4%
10	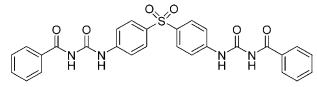	(**7.10** ± 1.04)[b]	56.8%
11	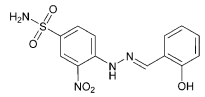	**9.46** ± 2.00	99.4%
12	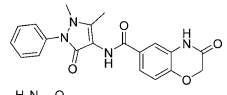	**50.9** ± 12.8	100%
13	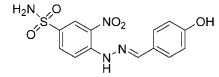	**8.03** ± 0.61	99.8%
14	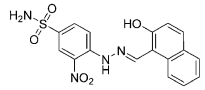	**6.54** ± 0.26	96.3%
15	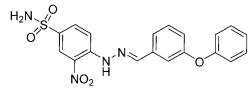	**3.99** ± 1.46	97.7%
16	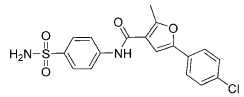	**45.1** ± 6.2	100%
17	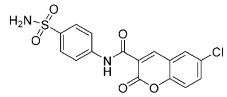	**1.90** ± 0.21	91.6%
18	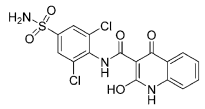	**15.5** ± 3.7	93.3%
19	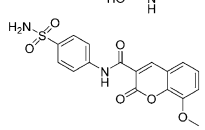	**16.6** ± 2.6	98.4%
20	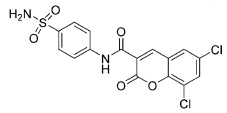	**74.8** ± 8.3	91.3%
21	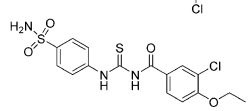	**46.5** ± 2.7	90.6%

[a]Compound structures were confirmed by HPLC-electrospray ionization mass spectrometry and purity was determined by HPLC-UV at 220−400 nm (see Experimental Section). [b]IC_{50} value is unreliable due to low purity of the test compound.

and therefore charged at physiological pH values. Thus, these compounds do not possess the properties required for orally bioavailable drugs.

To identify new inhibitors of *ecto*-5′-NT, we have applied a combination of similarity searching, flexible ligand docking into a carefully built comparative model of the enzyme, and intensive visual inspection and chemical interpretation of modeled complexes. The latter evaluation steps were critical for the selection of candidate compounds. This is further supported by the observation that the majority of newly identified inhibitors did not achieve high docking ranks, owing to the limitations of current scoring and ranking schemes. In

dx.doi.org/10.1021/jm300658n | J. Med. Chem. 2012, 55, 6576−6581

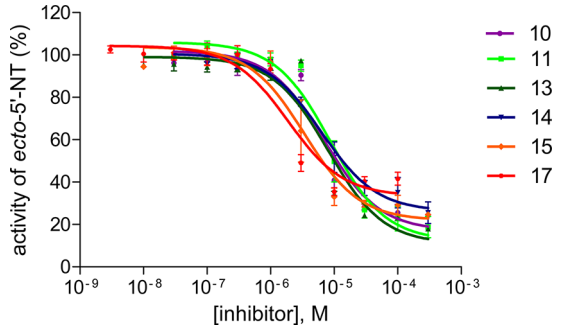

Figure 3. Concentration−inhibition curves. For newly identified *ecto*-5′-NT inhibitors with IC_{50} values below 10 μM, inhibition curves are shown. Compound numbers are listed on the right.

the case of *ecto*-5′-NT, an additional complication for docking analysis is provided by the location of the active side region at the interface between the two domains of the enzyme. Relative domain motions are likely in *ecto*-5′-NT, and it is thus not certain whether or not the model might closely resemble a substrate- or inhibitor-bound form of the enzyme. However, it has been encouraging that 13 of 51 selected candidates were found to be at least moderately potent inhibitors of *ecto*-5′-NT. Moreover, six of these compounds were active in the low micromolar range. Their level of potency is comparable to currently known anthraquinone-based inhibitors.

Most of the newly identified hits consisted of two moieties including a nucleoside-mimicking heterocycle or a substituted benzene and, in addition, a sulfonamide group (that very likely interacts with an active site zinc cation). These moieties were connected either by an amide, a hydrazone, or a urea linker. All of the compounds were drug-like, neutral molecules expected to show peroral absorption.

The newly identified inhibitors are accessible through well-established synthetic chemistry routes and amenable to synthesis of combinatorial compound arrays. Thus, there is considerable potential for further chemical exploration and optimization. Except for **10**, all newly identified inhibitors have a molecular weight lower than 430 Da and favorable ligand efficiency values (data not shown), providing a meaningful basis for further chemical exploration. Hence, taken together, the compounds might well be considered as first-in-class inhibitors of *ecto*-5′-NT, a highly attractive drug target.

CONCLUSIONS

With the aid of in silico compound screening, new inhibitors of *ecto*-5′-NT have been identified that are considered first-in-class from a medicinal chemical perspective. A total of 13 compounds were confirmed to be inhibitors of *ecto*-5′-NT. The most potent compounds contained sulfonamide groups and showed IC_{50} values in the low micromolar range and a competitive mechanism of inhibition. Compared to currently known active compounds, these newly identified inhibitors are thought to have significant potential for further development.

EXPERIMENTAL SECTION

Model Building. A sequence search using rat *ecto*-5′-NT, which was available to us for experimental testing, as a template was carried out in the Protein Data Bank.[15] The sequence searches identified two related enzymes with known X-ray structures. These structures included the 5′-nucleotidase precursor from *Thermus thermophilus* of HB8 (PDB code 2Z1A, ∼35% sequence identity; 1.75 Å crystallographic resolution)[15] and the 5′-nucleotidase from *Escherichia coli* (PDB code 1HPU, ∼25% sequence identity; 1.85 Å resolution).[1] Both structures were available in complexes with nucleoside inhibitors. We selected the *Thermus thermophilus* structure, having higher sequence similarity as a template for modeling after removal of the bound inhibitor. A structure-oriented sequence alignment of rat *ecto*-5′-NT and the 5′-nucleotidase precursor from *Thermus thermophilus* was carried out by including information from multiple other nucleotidase sequences. On the basis of this alignment, conserved regions were copied to the model and side chains of nonconserved residues and loops were modeled using the Molecular Operating Environment (MOE 2007.9).[16] Intramolecular contacts were regularized using limited energy minimization. Ramachandran plot[17] (Figure S2 of the Supporting Information) and PROSA II[18,19] profile analysis (Figure S3 of the Supporting Information) confirmed the stereochemical quality and sequence−structure compatibility of the model, respectively.

Virtual Screening. We applied a three-step virtual screening and compound selection strategy including similarity searching, docking, and extensive visual analysis. Initially, we reduced the ZINC-8 database[20] to a subset of compounds that displayed limited chemical similarity to the known active compounds in Figure 1. For this purpose, a 1-NN similarity search[21] using the reference compounds and MACCS structural keys[22] as a fingerprint was carried out. A total of 70000 database compounds were preselected beginning at a value of the Tanimoto coefficient (Tc)[23] of maximally 0.80 compared to the single most similar reference compound. Relative to the references, the preselected compounds spanned a Tc interval of [0.80−0.63]. In the second step, these 70000 database compounds were flexibly docked into the active site of the *ecto*-5′-NT model using FlexX.[24] In these calculations, FlexX default parameters were applied, except that the maximum overlap volume was increased from 2.9 to 5.0 Å^3 in order to mimic an induced fit effect during docking. On the basis of the

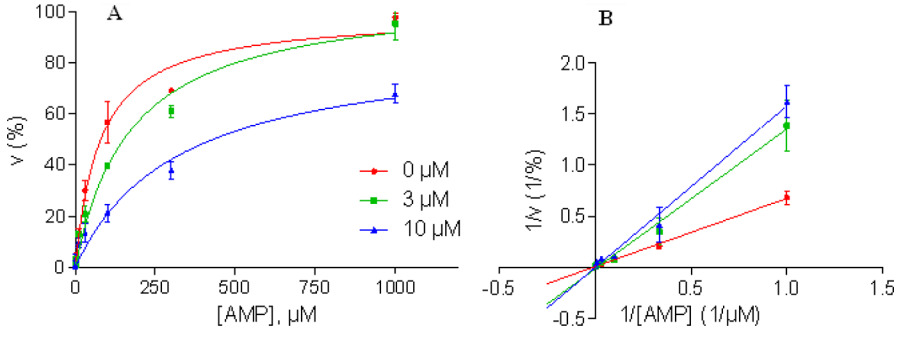

Figure 4. Determination of the inhibition mechanism of compound **17**. (A) Michaelis−Menten and (B) Lineweaver−Burk diagram of *ecto*-5′-NT inhibition in the absence (red) or presence of **17** at concentrations of 3 μM (green) and 10 μM (blue). Velocity values were normalized relative to V_{max} in the absence of inhibitor.

dx.doi.org/10.1021/jm300658n | J. Med. Chem. 2012, 55, 6576−6581

observed FlexX score distribution, 2700 compounds with most favorable docking scores were selected and subjected to initial inspection. In the first path, compounds were prioritized that displayed a complete or nearly complete fit into the active site of the model, leading to the selection of 372 candidates for further analysis.

In Vitro Assay. Candidate compounds were tested using a radioactive assay employing [^{3}H]AMP as a substrate. Purified recombinant rat *ecto*-5′-NT was used as previously described.[14,25,26] Assays were carried out with a substrate concentration of 5 μM (close to the K_m value). Compounds were initially tested at 100 and 10 μM concentration. For potent compounds, full concentration−response curves were obtained and IC_{50} values were determined. For examining the mechanism of inhibition, 10 different substrate concentrations were incubated with three different inhibitor concentrations. Data were analyzed using GraphPad Prism 5.0 (GraphPad Software Inc., San Diego, CA, USA). Curves were fitted by nonlinear regression using the Marquardt method[27] as implemented in GraphPad Prism. The K_i value of compound **17** was determined on the basis of its IC_{50} value using the Cheng−Prusoff equation.[28]

Purity Determination. The purity of active compounds was determined by HPLC coupled to electrospray ionization mass spectrometry (ESI-MS, Applied Biosystems API 2000; LCMS/MS, HPLC Agilent 1100) using the following procedure: stock solutions (10 μL) of compounds in DMSO were diluted with 40 μL of MeOH containing 2 mM NH_4CH_3COO. Then 10 μL of the sample was injected into an HPLC column (Macherey + Nagel EC 50/2 Nucleodur C18 Gravity 3 μM). Elution was performed with a gradient of 60:40 to 0:100 for 10 min at a flow rate of 300 μL/min, starting the gradient directly. UV absorption was detected from 190 to 900 nm using a diode array detector. The purity of the compounds was determined at 220−400 nm.

■ ASSOCIATED CONTENT

Supporting Information

Source information and docking ranks of active compounds and concentration−inhibition curves, a Ramachandran diagram of the *ecto*-5′-NT molecular model, and a PROSA II profile. This material is available free of charge via the Internet at http://pubs.acs.org.

■ AUTHOR INFORMATION

Corresponding Author

*For J.B.: phone, +49-228-2699-306; fax, +49-228-2699-341; E-mail, bajorath@bit.uni-bonn.de. For C.E.M.: phone, +49-228-73-2301; fax, +49-228-73-2567; E-mail, christa.mueller@uni-bonn.de.

Present Address

‖Institute of Pharmaceutical Sciences, ETH Zürich, HCI H437, Wolfgang-Pauli-Strasse 10, CH-8092 Zürich, Switzerland.

Notes

The authors declare no competing financial interest.

■ ACKNOWLEDGMENTS

We thank Martin Vogt and Ruifang Li for helpful discussions, Nicole Florin, Inês da Fonseca Santos Ferreira, and Gerard Murphy for preliminary enzyme inhibition experiments, and Marion Schneider for LCMS measurements.

■ ABBREVIATIONS USED

AMP, ADP, and ATP, adenosine mono-, di-, and triphosphate; AMPCP, α,β-methylene-ADP; *ecto*-5′-NT, *ecto*-5′-nucleotidase; HPLC, high performance liquid chromatography; ESI-MS, electrospray ionization mass spectrometry; LCMS, liquid chromatography mass spectrometry; SEM, standard error of the mean

■ REFERENCES

(1) Knöfel, T.; Sträter, N. Mechanism of hydrolysis of phosphate esters by the dimetal center of 5′-nucleotidase based on crystal structures. *J. Mol. Biol.* **2001**, *309*, 239−254.
(2) Sträter, N. *ecto*-5′-nucleotidase: structure−function relationships. *Purinergic Signalling* **2006**, *2*, 343−350.
(3) Zimmermann, H. 5′-Nucleotidase: molecular structure and functional aspects. *Biochem. J.* **1992**, *285*, 345−365.
(4) Zimmermann, H.; Zebisch, M.; Sträter, N. Cellular function and molecular structure of *ecto*-nucleotidases. *Purinergic Signalling* **2012**, *8*, 437−502.
(5) Colgan, S. P.; Eltzschig, H. K.; Eckle, T.; Thompson, L. F. Physiological roles for *ecto*-5′-nucleotidase (CD73). *Purinergic Signalling* **2006**, *2*, 351−360.
(6) Fredholm, B. B.; IJzerman, A. P.; Jacobson, K. A.; Linden, J.; Müller, C. E. International Union of Basic and Clinical Pharmacology. LXXXI. Nomenclature and classification of adenosine receptors. *Pharmacol. Rev.* **2011**, *63*, 1−34.
(7) Deaglio, S.; Robson, S. C. Ectonucleotidases as regulators of purinergic signalling in thrombosis, inflammation, and immunity. *Adv. Pharmacol.* **2011**, *61*, 301−332.
(8) Buchheiser, A.; Ebner, A.; Burghoff, S.; Ding, Z.; Romio, M.; Viethen, C.; Lindecke, A.; Köhrer, K.; Fischer, J. W.; Schrader, J. Inactivation of CD73 promotes atherogenesis in apolipoprotein E-deficient mice. *Cardiovasc. Res.* **2011**, *92*, 338−347.
(9) El-Tayeb, A.; Iqbal, J.; Behrenswerth, A.; Romio, M.; Schneider, M.; Zimmermann, H.; Schrader, J.; Müller, C. E. Nucleoside-5′-monophosphates as prodrugs of adenosine A_{2A} receptor agonists activated by *ecto*-5′-nucleotidase. *J. Med. Chem.* **2009**, *52*, 7669−7677.
(10) Stagg, J.; Divisekera, U.; McLaughlin, N.; Sharkey, J.; Pommey, S.; Denoyer, D.; Dwyer, K. M.; Smyth, M. J. Anti-CD73 antibody therapy inhibits breast tumor growth and metastasis. *Proc. Natl. Acad. Sci. U.S.A.* **2010**, *107*, 1547−1552.
(11) Clayton, A.; Al-Taei, S.; Webber, J.; Mason, M. D.; Tabi, Z. Cancer exosomes express CD39 and CD73, which suppress T cells through adenosine production. *J. Immunol.* **2011**, *187*, 676−683.
(12) Stagg, J.; Divisekera, U.; Duret, H.; Sparwasser, T.; Teng, M. W. L.; Darey, P. K.; Smyth, M. J. CD73-deficient mice have increased antitumor immunity and are resistant to experimental metastasis. *Cancer Res.* **2011**, *71*, 2892−2900.
(13) Stagg, J.; Beavis, P. A.; Divisekera, U.; Liu, M. C. P.; Möller, A.; Darcy, P. K.; Smyth, M. J. CD73-deficient mice are resistant to carcinogenesis. *Cancer Res.* **2012**, *72*, 2190.
(14) Baqi, Y.; Lee, S.-Y.; Iqbal, J.; Ripphausen, P.; Lehr, A.; Scheiff, A. B.; Zimmermann, H.; Bajorath, J.; Müller, C. E. Development of potent and selective inhibitors of *ecto*-5′-nucleotidase based on an anthraquinone scaffold. *J. Med. Chem.* **2010**, *53*, 2076−2086.
(15) Bernstein, F. C.; Koetzle, T. F.; Williams, G. J.; Meyer, E. E., Jr.; Brice, M. D.; Rodgers, J. R.; Kennard, O.; Shimanouchi, T.; Tasumi, M. The Protein Data Bank: a computer-based archival file for macromolecular structures. *J. Mol. Biol.* **1977**, *112*, 535−542.
(16) *Molecular Operating Environment (MOE 2007.09)*; Chemical Computing Group: Montreal, Quebec, Canada, 2007.
(17) Ramachandran, G. N.; Ramakrishnan, C.; Sasisekharan, V. Stereochemistry of polypeptide chain configurations. *J. Mol. Biol.* **1963**, *7*, 95−99.
(18) Sippl, M. J. Recognition of errors in three-dimensional structures of proteins. *Proteins* **1993**, *17*, 355−362.
(19) Wiederstein, M.; Sippl, M. J. ProSA-web: interactive web service for the recognition of errors in three-dimensional structures of proteins. *Nucleic Acids Res.* **2007**, *35*, 407−410.
(20) Irwin, J. J.; Shoichet, B. K. ZINC. A free database of commercially available compounds for virtual screening. *J. Chem. Inf. Model.* **2005**, *45*, 177−182.
(21) Schuffenhauer, A.; Floersheim, P.; Acklin, P.; Jacoby, E. Similarity metrics for ligands reflecting the similarity of the target proteins. *J. Chem. Inf. Comput. Sci.* **2003**, *43*, 391−405.
(22) *MACCS Keys*; MDL Information Systems Inc.: San Leandro, CA, 2005; http://www.mdl.com.

(23) Willett, P. Similarity-based virtual screening using 2D fingerprints. *Drug Discovery Today* **2006**, *11*, 1046−1053.
(24) *FlexX*; BioSolveIT GmbH: An der Ziegelei 79, 53757 Sankt Augustin, Germany, 2008.
(25) Servos, J.; Reiländer, H.; Zimmermann, H. Catalytically active soluble *ecto*-5′-nucleotidase purified after heterologous expression as a tool for drug screening. *Drug Dev. Res.* **1998**, *45*, 269−276.
(26) Iqbal, J.; Jirovsky, D.; Lee, S.-Y.; Zimmermann, H.; Müller, C. E. Capillary electrophoresis-based nanoscale assays for monitoring *ecto*-5′-nucleotidase activity and inhibition in preparations of recombinant enzyme and melanoma cell membranes. *Anal. Biochem.* **2008**, *373*, 129−140.
(27) Marquardt, D. W. An algorithm for least squares estimation of non-linear parameters. *J. Soc. Indust. Appl. Math.* **1963**, *11*, 431−441.
(28) Cheng, Y.-C.; Prusoff, W. H. Relationship between the inhibition constant (K_i) and the concentration of inhibitor which causes 50% inhibition (I_{50}) of an enzymatic reaction. *Biochem. Pharmacol.* **1973**, *22*, 3099−3108.